Available online at www.sciencedirect.com
SCIENCE DIRECT®
International Journal of Refrigeration 28 (2005) 859–871
REVUE INTERNATIONALE DU FROID
INTERNATIONAL JOURNAL OF
refrigeration
www.elsevier.com/locate/ijrefrig

A novel experimental investigation of a solar cooling system in Madrid

A. Syed[a,b], M. Izquierdo[d,*], P. Rodríguez[e], G. Maidment[b], J. Missenden[b], A. Lecuona[e], R. Tozer[b,c]

[a]*Cundall Johnston and Partners LLP Consulting Engineers, 13–17 Long Lane, EC1A 9RH London, UK*
[b]*London South Bank University, Faculty of Engineering, Science and the Built Environment, 103 Borough Road, SE1 0AA London, UK*
[c]*Waterman Gore Consulting Engineers, Versailles Court, 3 Paris Garden, SE1 8ND London, UK*
[d]*Instituto de Ciencias de la Construcción Eduardo Torroja (CSIC), c/ Serrano Galavache S/no. 28033, Madrid, España*
[e]*Universidad Carlos III de Madrid, Escuela Politécnica Superior, Avenida de la Universidad 30, 28911 Leganés, Madrid, España*

Received 12 January 2004; received in revised form 3 January 2005; accepted 25 January 2005
Available online 22 March 2005

Abstract

This paper reports novel experimental results derived through field testing of a part load solar energized cooling system for typical Spanish houses in Madrid during the summer period of 2003. Solar hot water was delivered by means of a 49.9 m^2 array of flat-plate collectors to drive a single-effect ($LiBr/H_2O$) absorption chiller of 35 kW nominal cooling capacity. Thermal energy was stored in a 2 m^3 stratified hot water storage tank during hours of bright sunshine. Chilled water produced at the evaporator was supplied to a row of fan coil units and the heat of condensation and absorption was rejected by means of a forced draft cooling tower. Instantaneous, daily and period energy flows and energy balance in the installation is presented. System and absorption machine temperature profiles are given for a clear, hot and dry day's operation. Daily and period system efficiencies are given. Peak insolation of 969 W m^{-2} (at 12:30 solar time on 08/08/03) produced 5.13 kW of cooling at a solar to cooling conversion efficiency of 11%. Maximum cooling capacity was 7.5 kW. Cooling was provided for 8.67 h and the chiller required a threshold insolation of 711 W m^{-2} for start-up and 373 W m^{-2} for shut-down. A minimum hot water inlet temperature to the generator of 65 °C was required to commence cold generation, whereas at 81 °C, 6.4 kW of cooling (18.3% of nominal capacity) was produced. The absorption refrigeration machine operated within the generation and absorption temperature ranges of 57–67 and 32–36 °C, respectively. The measured maximum instantaneous, daily average and period average COP were 0.60 (at maximum capacity), 0.42 and 0.34, respectively. Energy flows in the system are represented on a novel area diagram. The results clearly demonstrate that the technology works best in dry and hot climatic conditions where large daily variations in relative humidity and dry bulb temperature prevail. This case study provides benchmark data for the assessment of other similar prototypes and for the validation of mathematical models.

Keywords: Air conditioning; Residential building; Spain; Experiment; Absorption system; Water-lithium bromide; Solar collector; Thermal storage

* Corresponding author. Fax: +34 91 8713248.
E-mail address: mizquierdo@ietcc.csic.es (M. Izquierdo).

0140-7007/$35.00 © 2005 Elsevier Ltd and IIR. All rights reserved.
doi:10.1016/j.ijrefrig.2005.01.007

Etude expérimentale sur un système de refroidissement solaire innovant à Madrid

Mots clés : Conditionnement d'air ; Immeuble résidentiel ; Espagne ; Expérimentation ; système à absorption ; Eau-bromure de lithium ; Capteur solaire ; Accumulation thermique

1. Introduction

The incidence of solar energy and cooling requirements are approximately in phase, which makes solar cooling an attractive alternative to conventional (electric) cooling in modern buildings.

A few contemporary investigators have demonstrated solar air-conditioning by energizing single-effect ($LiBr/H_2O$) absorption machines with heat of flat-plate collectors operating between 70 and 90 °C [1–5]. Recent technical improvements in collectors [6] and sorption cycles [7] have presented opportunities for improved performance of solar cooling systems. Since the collector cost ranges from 50 to 80% of the system cost and is highly temperature sensitive, sorption cycles energized at lower driving temperature are more economical [8]. When the sun is used as the only heat source with thermal storage, these systems are characterized as having high collector efficiency, part load operation, high COP [9] and long daily cooling periods. Higher COP, cooling capacity and longer daily cooling periods can be

Nomenclature

A	absorber area (m^2)
COP	coefficient of performance (–)
C_p	specific heat capacity of water (4.18 kJ kg^{-1} K^{-1})
G	global (horizontal) insolation (W m^{-2})
$\dot{m}$	mass flow rate (kg s^{-1})
N	sample size (–)
$\dot{Q}$	heat (kW)
q	heat flux (W m^{-2})
RH	relative humidity (%)
SCOP	solar coefficient of performance (–)
SCR	solar cooling ratio (–)
S_X	standard deviation (–)
T	temperature (°C)
X	characteristic parameter for collector efficiency plot (m^2 K W^{-1})
X_i	single reading (–)
$\bar{X}$	mean of the sample (–)
x_{max}	maximum allowable deviation about mean (–)

Greek symbols

ε	effectiveness
η	efficiency
τ	deviation from mean value

Subscripts

a	absorber
a,loss	absorption machine loss
c	condenser
cw	cooling water
chw	chilled water
db	dry bulb
e	evaporator
echw	entering chilled water
ecw	entering cooling water
efpc	entering flat-plate collector
ehw	entering hot water
ehxpc	entering heat exchanger in primary circuit
etsc	entering tank in secondary circuit
ettc	entering tank in tertiary circuit
eg	entering generator
ea	entering absorber
la	leaving absorber
fpc	flat-plate collector
g	generator
lchw	leaving chilled water
lcw	leaving cooling water
lfpc	leaving flat-plate collector
lhw	leaving hot water
lhxpc	leaving heat exchanger in primary circuit
lhxsc	leaving heat exchanger in secondary circuit
ltsc	leaving tank in secondary circuit
lttc	leaving tank in tertiary circuit
pcw	primary circuit water
scw	secondary circuit water
shx	solution heat exchanger
T	tilted
t,input	tank input
t,loss	tank loss
t,output	tank output
t,stored	tank stored
tcw	tertiary circuit water

achieved with evacuated tube collector systems operating up to 170 °C with high efficiencies [10]. However, their life-cycle costs are much higher than a conventional chiller system [11].

A state-of-the-art solar cooling system consisting of a 35 kW LiBr/H_2O absorption machine energized by 49.9 m^2 of flat-plate collectors was experimentally investigated in Madrid during the summer period of 2003. The need for the investigation arose from the requirement to optimise system design, [12,13]. Experimental validation of mathematical models is a prerequisite to system optimisation, which necessitate the acquisition of accurate data from specific installations. With much diffusion and lack of coherent industry standards to rate solar cooling equipment, a consistent and reliable operating data set was difficult to obtain from published literature. Hence this investigation was commissioned.

The research objectives were as follows:

- To provide a coherent data set consisting of instantaneous, daily and period results of heat flows and energy balance in a real solar cooling system.
- To gain an understanding of the significance and location of heat losses in the system.
- To develop a novel area representation of the global system operating on solar energy.
- To develop process and environmental temperature profiles.
- To assess the performance of the refrigeration plant under varying climatic conditions.
- To compute the instantaneous, daily and period system efficiencies.

In what follows, the whole experimental facility and individual system components are described with the methodology used for testing these under real time conditions. Results, discussion and energy balance analysis is then presented. Following from the results, key conclusions are drawn along with recommendations to improve the process efficiencies.

2. Description of the experimental plant

A solar powered air-conditioning system designed for heating and cooling typical Spanish houses of average occupied area of 80 m^2 in Madrid was recently put into operation at Carlos III University of Madrid, using commercially available components. The investigators using the technology responded to the need of potential users to gain confidence on its performance, operative characteristics, and to perform experimental research. It was funded with collaboration between the Spanish Ministry of Industry, the local government of Madrid, the Carlos III University and the Instituto Eduardo Torroja de Ciencias de la Construcción (IETcc), belonging to CSIC.

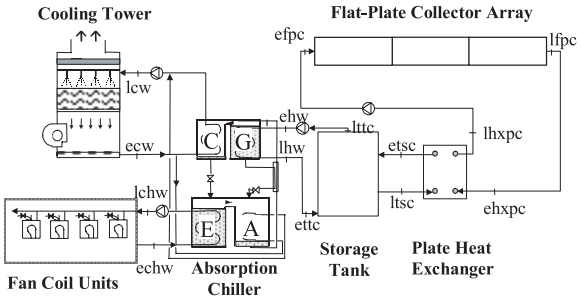

ecw : entering cooling water
lcw : leaving cooling water
echw : entering chilled water
lchw : leaving chilled water
efpc : entering flat-plate collector
lfpc : leaving flat-plate collector
ehw : entering hot water
lhw : leaving hot water
etsc : entering tank at secondary circuit
ltsc : leaving tank at secondary circuit
ettc : entering tank at tertiary circuit
lttc : leaving tank at tertiary circuit
ehxpc : entering heat exchanger at primary circuit
lhxpc : leaving heat exchanger at primary circuit
A : Absorber ; C : Condenser ; E : Evaporator ; G : Generator

Fig. 1. The Carlos III university solar cooling scheme.

Fig. 1 shows a schematic of the experimental solar absorption air-conditioning plant consisting of four main water streams flowing though the generator, evaporator, condenser and absorber. Twenty flat-plate collector modules with an absorber area of 2.5 m^2 each were used to energize the system. The individual collector modules were connected sharing the same manifold, however the rows of collectors were connected in parallel to keep the pressure drop low in the circuit. Pressure drop and pumping energy has been previously shown by Syed et al. [8] as being a controlling factor in solar cooling scheme economics. 28 mm copper pipes were provided in the main primary circuit and the row connections were made up of 22 mm copper pipes. The collectors supplied heat to a 2 m^3 storage tank via a plate heat exchanger.

Primary hot water was circulated through the flat-plate collector panels and heated up to 90 °C by incidence of solar energy on the copper absorber plates. The heat produced was transferred to a storage tank via a plate heat exchanger. At about 80 °C prevailing at the top of the tank, heat was supplied to the generator of a 35 kW nominal cooling capacity (LiBr/H_2O) absorption chiller, which operated in vacuum. This was to boil a weak solution of solvent and refrigerant (lithium bromide and water), that resulted in a strong solution. The refrigerant vapour was condensed on the condenser tubes. The condensate was throttled through an expansion device obtaining two-phase refrigerant; the liquid refrigerant evaporated under low pressure in the evaporator, thus producing cooling. Chilled water flowing through the evaporator tubes was supplied to the fan coil units at about 8 °C. Meanwhile, the strong solution from the generator passed through a counter flow heat exchanger to preheat the weak solution entering the generator. In the

absorber, the refrigerant vapour from the evaporator was absorbed in the strong solution. The heat of condensation and absorption was removed from the system by means of cooling water entering/leaving the chiller at about 20/25 °C flowing through the tubes of the absorber and condenser in parallel connected to a forced draft cooling tower. The solution was circulated by thermosyphon principle, therefore the chiller design did not incorporate a mechanical pump. However, pumps were used to circulate water between the collector array and the plate heat exchanger, plate heat exchanger and storage tank, storage tank and generator, cooling tower and absorber/condenser and fan coil units and evaporator. Thermal energy was supplied entirely by solar collectors.

3. Experimental procedure

During the period of investigation of 20 days in the summer of 2003, the hours of bright sunshine were accompanied with high dry bulb temperature and lower relative humidity (at a wet bulb temperature of about 18 °C). Under such environmental conditions, heat was stored in the tank when the collector outlet water temperature exceeded the average tank temperature by 2–3 °C. Conversely, the primary (collector) circuit was isolated from the tank, so only the heat stored in the tank was supplied to the generator of the absorption chiller until no further cooling could be produced.

Fig. 2 shows a view of the collector array and Fig. 3(a)–(d), shows the absorption chiller, cooling tower, storage tank and plate heat exchanger. The following subsections describe these components in more detail and present methods for testing them under real time conditions.

3.1. Solar collectors

The flat-plate collector panels were supplied with a selective sol-titanium (TiNox) coating on a copper substrate.

Fig. 2. View of the flat-plate solar collector array installed on the roof of UC3M Leganés Campus.

This combination produced high absorptive and low emissive properties [14]. A serpentine copper tube brazed to the sheet was provided to accommodate the flow of hot water. To ensure hydraulic balance, the collector field was split into four rows of six, six, five and three panels. The row lengths were 15.85, 15.58, 12 and 7.19 m. The tilt was approximately 40° and the azimuth was due South. Safety release valves and check valves were installed in each row to avoid reverse flow and high-pressure buildup. Also, the collector pump was made to circulate hot water continuously to ensure that the collectors operated well below their stagnation temperature.

The collector efficiency was measured outdoors for a range of inlet and outlet temperatures, dry bulb temperatures, solar insolation and primary circuit flow rates. Fig. 4 shows the instantaneous experimental collector efficiency plot of the data acquired at solar noon on 62 clear days from 6th June to 18th August 2003. To derive the collector efficiency Eq. (2), the inlet and outlet collector water temperatures and flow rates were measured as well as the insolation at normal transmittance and absorptance of incident light and dry bulb temperatures. The following efficiency equation was used:

$$\eta_{\mathrm{fpc}} = \frac{\dot{m}_{\mathrm{pcw}} C_{\mathrm{p}} (t_{\mathrm{lfpc}} - t_{\mathrm{efpc}})}{G A_{\mathrm{fpc}}} \tag{1}$$

Linear regression through the data points on Fig. 4 is shown by a solid line, which has the equation:

$$\eta_{\mathrm{fpc}} = 77.43 - 344.9X \tag{2}$$

where

$$X = \frac{\frac{t_{\mathrm{efpc}} + t_{\mathrm{lfpc}}}{2} - t_{\mathrm{db}}}{G} \tag{3}$$

The correlation coefficient (R^2 value) for Eq. (2) is 0.58, which may seem low however it satisfies the Chauvenet's Criterion for the elimination of widely scattered data points [15]. The non-dimensional deviation about the mean value τ was found for each reading from the following equation:

$$\tau = \frac{X_i - \bar{X}}{S_X} \tag{4}$$

The standard deviation S_X was determined by:

$$S_X = \sqrt{\frac{\sum_{i=1}^{n} (X_i - \bar{X})^2}{N - 1}} \tag{5}$$

The τ value of each reading was compared with the ratio of the maximum allowable deviation from the mean value and standard deviation (x_{max}/S_X) which depends on the sample size [15]. A datum falling outside the allowable range of x_{max}/S_X was removed in two successive trials by computing the statistics for each trial. As a result, two points from an initial sample size of 64 were removed by applying the Criterion.

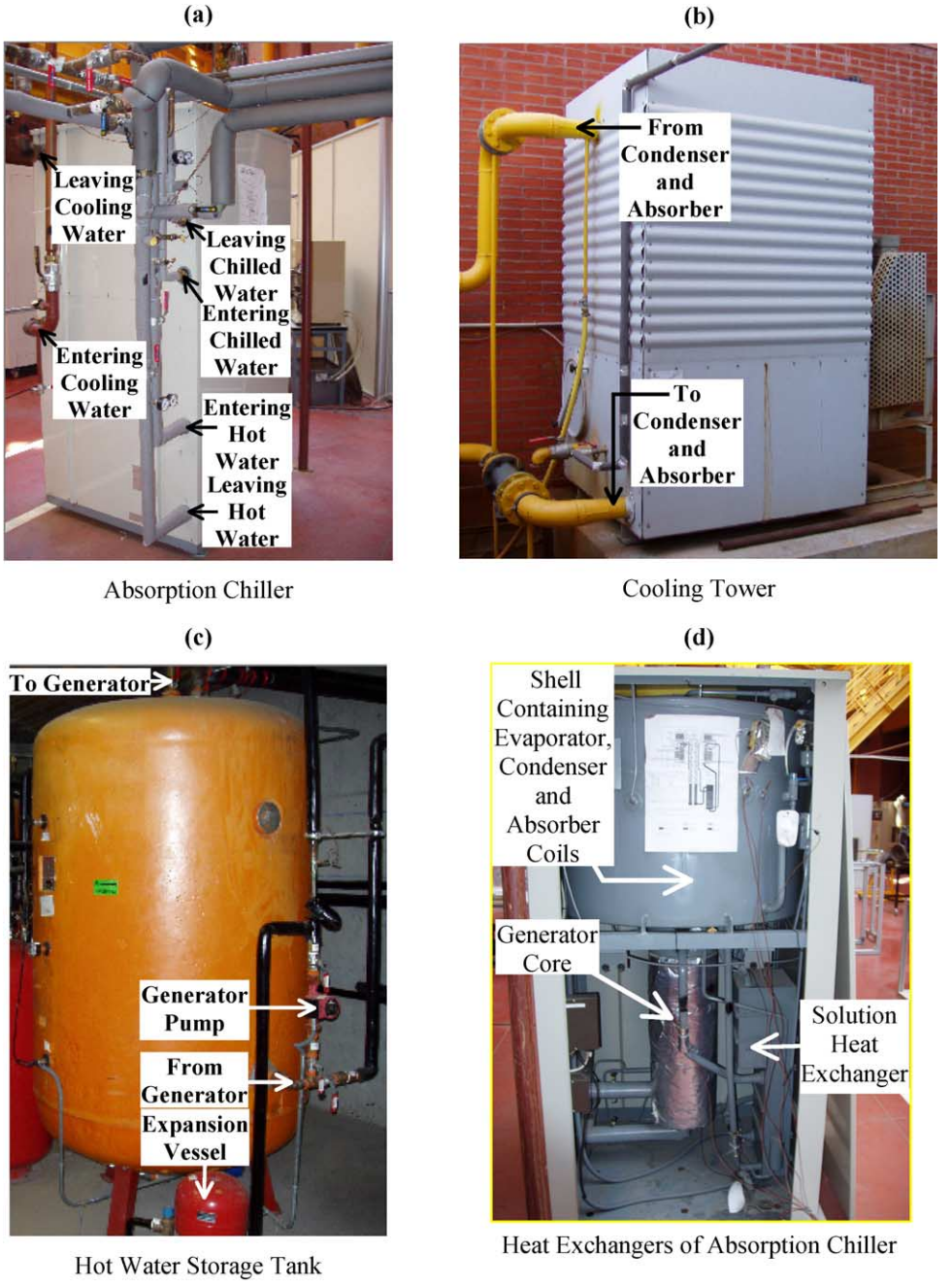

Fig. 3. (a) Absorption chiller; (b) cooling tower; (c) storage tank; (d) heat exchangers of absorption chiller.

The range of measurement uncertainty was found to be $\pm 1.91\%$, shown by the dashed lines on Fig. 4. This was determined for T_{efpc}, ΔT_{fpc}, T_{db}, $\dot{m}_{pcw}$, A_{fpc} within the limits of ISO 9806-1 [16] and G for a class 1 pyranometer [17] within the limits of ISO 9060 [18] by applying the root sum squares of the instrument errors.

A comparison was made between the efficiency plots generated with the coefficients provided by a collector certifying authority [14] and our real test data, which showed small differences as indicated on Fig. 4. This validated the test data and confirmed that the measurement and data acquisition system were highly accurate.

3.2. Storage tank

The use of a hot water tank between the collector and the

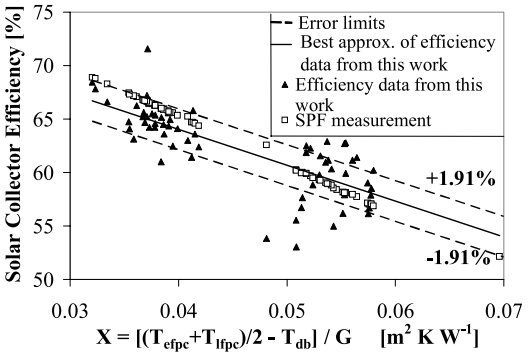

Fig. 4. Experimentally derived collector efficiency data and regression straight line for the installed flat-plate collectors.

absorption machine has been reported to yield higher system efficiency [5] and extends the daily cooling period. It also prevents cycling of the absorption machine due to variations in solar radiation intensity. In the mornings, the process of heat addition to the tank was initiated when the insolation was between 500 and 600 W m^{-2} and the temperature output from the collector was higher than the average tank temperature by 2–3 °C. At 08:30 (solar time, 1 h: 1 min) on the morning of 08/08/03, the tank valves were opened and the generator pump was switched on to allow the flow of hot water into the generator. In the evenings, the decision to isolate the tank from the collectors (by closing the tank valves) to utilise the stored heat was made when the insolation reduced below 550 W m^{-2}. Further work is required to identify optimum storage and startup protocols. Circulation between the tank and the generator was maintained until the entering and leaving hot water temperature difference at the generator reduced to 1 °C or lower.

The useful solar heat input to the tank was determined with the measured flow rate in the secondary hot water circuit (between the plate heat exchanger and the tank) and the temperature difference across the inlet and outlet of the tank by applying:

$$\dot{Q}_{t,input} = \dot{m}_{scw} C_p \left(t_{etsc} - t_{ltsc}\right) \quad (6)$$

Similarly, the heat output from the tank was evaluated by applying the same form of equation to the tertiary hot water circuit (connecting the tank to the generator) as follows:

$$\dot{Q}_{t,output} = \dot{m}_{tcw} C_p \left(t_{lttc} - t_{ettc}\right) \quad (7)$$

The heat loss from the storage tank was found to be a significant contributing factor to the heat loss from the system to the environment. Applying energy balance on the tank the equation of following form was obtained:

$$Q_{t,input} + Q_{t,stored} = Q_{t,loss} + Q_{t,output} \quad (8)$$

To minimize the tank loss, a fiberglass insulating material with a thickness of 50–60 mm has been recommended, which yields an overall heat loss coefficient (U value) of 0.5–0.9 W m^{-2} K^{-1}. Again, optimum storage characteristics are subject of future work.

3.3. Absorption chiller

A 35 kW nominal cooling capacity indirect hot water driven WFC-10 absorption chiller manufactured by Yazaki [19] was used, since a commercial product with a cooling capacity of 10 kW was not available.

The generator design of the machine allowed the use of hot water in the temperature range of 65–90 °C. Cold production was observed to begin when the temperature at the uppermost part of the tank reached 65 °C. The measured volumetric flow rate of hot water delivered by generator pump was about 0.28 l s^{-1}. Since the temperature of hot water entering and leaving the generator was also measured, at any given time, the heat delivered to the generator was evaluated from the following equation:

$$\dot{Q}_g = \dot{m}_{tcw} C_p (t_{ehw} - t_{lhw}) \quad (9)$$

Nominal cooling capacity of 35 kW can be produced with this chiller at the following operating conditions:

- entering/leaving hot water temperature = 88/83 °C (at flow rate: 2.4 l s^{-1})
- entering/leaving cooling water temperature = 29.5/34.5 °C (at flow rate: 4.0 l s^{-1})
- leaving/entering chilled water temperature = 9/14 °C (at flow rate: 1.7 l s^{-1}).

Pumps supplying water to the generator, evaporator and absorbser–condenser heat exchangers were sized to deliver 25% of the nominal cooling capacity. An entering generator hot water temperature of 79 °C on 8th August 2003, resulted in a cooling capacity of 7.5 kW (21.4% of nominal capacity) (Table 1).

A fan coil unit (FCU) of 10 kW cooling capacity (28.6% of nominal capacity) was used to supply cold air into the laboratory space. A second FCU was used to regulate the chilled water temperature and provided a safety measure for ensuring that the evaporator temperature was kept above 4–5 °C at all times, irrespective of the cooling coil load. Lower evaporating temperatures can result in a freezing problem. The cooling coil was directly connected to the evaporator. The chilled water temperature was kept within 7–10 °C by thermostatic control. Measured chilled water flow rate was about 0.29 l s^{-1}. The entering and leaving chilled water temperatures were measured, which allowed the estimation of the evaporator load at any given time from the following equation:

$$\dot{Q}_e = \dot{m}_{chw} C_p \left(t_{echw} - t_{lchw}\right) \quad (10)$$

A cooling tower was used for rejecting the heat of absorption and condensation and supplied cooling water to the absorber and condenser in parallel at about 21 °C.

Table 1
Summary of results for the monitored day: 8th August 2003

Solar time (h:min)	Measured solar insolation (W m^{-2})	Measured entering generator hot water temperature (°C)	Measured leaving chilled water temperature (°C)	Observations	Cooling capacity [a] (kW)	COP (–)
08:30	478	58.7	26.3	Start of heat input of tank	–	–
09:40	711	65	29.5	Start of cold production	0.2	–
12:30	969	79	8.7	Peak solar insolation or peak heat input to tank	5.13	0.38
14:30	809	79.7	8	Equal tank heat output and input	6.63	0.51
14:50	752	79	8.1	Peak cooling produced	7.5	0.6
16:40	373	68.5	8.9	End of heat input to tank	4.95	0.61
18:20	53	61.6	16.4	End of cold production	1.03	0.37

[a] Nominal cooling capacity = 35 kW.

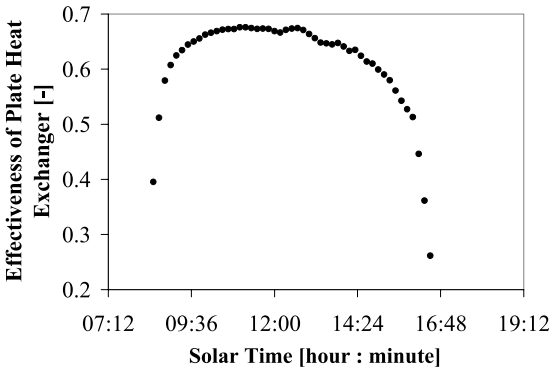

Fig. 5. Effectiveness of collector-tank plate heat exchanger against solar time (08/08/2003).

Crystallization problem was not encountered by supplying a low cooling water temperature. The measured flow rate of cooling water delivered by the condenser pumps was approximately 0.81 l s^{-1}. The cooling tower used was of open forced-draft type (fan located at the base of the unit). The total heat rejection rate was evaluated from the sum of the heat dissipated at the condenser and the absorber:

$$\dot{Q}_c + \dot{Q}_a = \dot{m}_{cw} C_p (t_{lcw} - t_{ecw}) \quad (11)$$

Eq. (12) is an energy balance relation applied to the main heat exchangers of the absorption machine. The result showed that the machine was operating near adiabatically, such that minor losses to the surroundings were found.

$$Q_g + Q_e = Q_c + Q_a + Q_{a,loss} \quad (12)$$

The refrigeration coefficient of performance (COP) was determined from the ratio of the evaporator load and generator load:

$$\mathrm{COP} = \frac{Q_e}{Q_g} \quad (13)$$

Although the COP varied widely during the day due to the chiller operating in transient regime, a maximum COP of 0.63 and an average of 0.42 was achieved for the period of cold production on 8th August 2003.

3.4. Plate heat exchanger

A plate heat exchanger located in the tank room was used to separate the primary and secondary water circuits. This was provided to operate the system in heating mode by adding propylene glycol in the primary circuit, which could not be allowed to mix with the tank water for public health reasons. The additive was removed for this investigation. An evaluation of the heat exchanger effectiveness was made with the following equation (with reference to Fig. 1):

$$\varepsilon = \frac{t_{etsc} - t_{ltsc}}{t_{ehxpc} - t_{ltsc}} \quad (14)$$

This parameter reduces the useful heat delivered by the solar collectors and is therefore desirable to be close to unity. The effectiveness varies with solar time, increasing and decreasing rapidly as the collector water temperature increases and decreases at the beginning and end of the day, respectively. For a major part of the period of heat input to tank on 08/08/03, from 08:30 to 16:30, the effectiveness was found to be between 0.6 and 0.7 as shown in Fig. 5.

4. Environmental parameters

Fig. 6 shows a plot of the environmental temperatures and relative humidity for 08/08/03, which affect the performance of the absorption machine and solar collectors. From Fig. 6, it can be seen that the relative humidity decreased significantly from 28.2% at 08:30 to 12.3% at

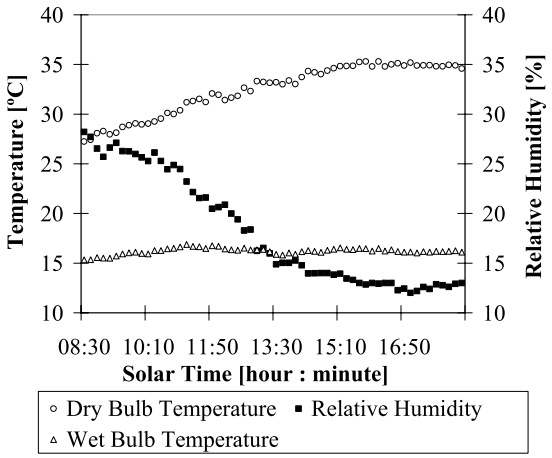

Fig. 6. Environmental temperature and relative humidity against solar time (08/08/2003).

16:40 where it stabilized until 17:10, followed by a small increase at the end of the cooling period. Conversely, the dry bulb temperature increased by 7.4 °C. Both these and atmospheric pressure data were used to determine the wet bulb temperature with EES software, found to be 15.3–16.9 °C. The temperature difference (approach) of the entering condensing water temperature and wet bulb temperature was hence determined. This was between 3.2 and 4.8 K from 09:40 to 18:20. In this period, the range (difference) of entering and leaving cooling water temperatures was found to be 3.3–5.5 K. Tozer and Lozano [20] found thermoeconomically optimum approach and range temperatures of 5 and 6 K, respectively, for 90/80 °C hot water, 21 °C wet bulb for a whole year of equivalent full load hours. As these optimum temperatures were approached the cooling capacity was found to increase significantly as shown in Fig. 7.

The main reason for the low wet bulb temperature was the low relative humidity in Madrid during peak cooling period.

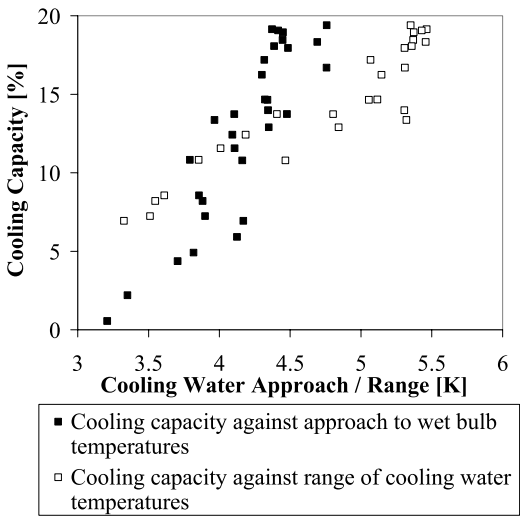

Fig. 7. Cooling capacity against approaches and ranges of cooling water (08/08/2003).

5. Process temperatures

Fig. 8 shows a plot of the temperatures of the water streams that flowed through the absorption chiller on 08/08/03. These temperatures have a strong impact on the COP and cooling capacity of the machine [21]. From the time the evaporator temperature started decreasing, the chiller entered transient regime of operation. This occurred at 09:40. When the leaving chilled water temperature reached 9 °C at 10:50, the chiller entered permanent regime, so the start-up duration of transient operation was 1.17 h. It operated under permanent regime until 18:10, for 7.33 h. The chiller once again entered transitory regime for a further 10 min until the leaving chilled water temperature exceeded 16 °C (at 18:20), as shown in Fig. 8.

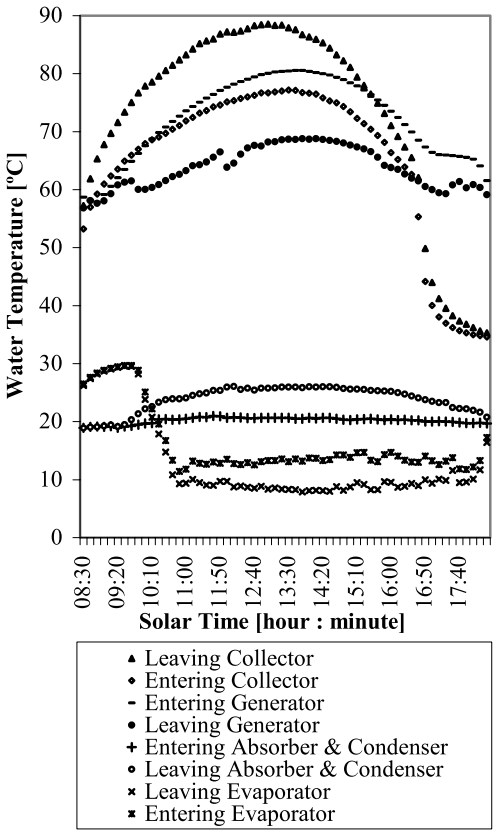

Fig. 8. Flow temperatures in water circuits against solar time (08/08/2003).

6. Results and discussion

The solar cooling system was tested daily from the 25th of July till the 19th of August 2003. During these days, the sky in Madrid was generally clear, thus ideal for solar cooling and permitted the use of clear sky models for the calculation of tilted insolation from the horizontal pyranometer reading [22]. In the present work, data from a hot sunny day on the 8th of August 2003 is presented in detail. This is because on this day, the highest cooling energy of 40 kW h day^{-1} was produced. The daily energy flows in the installation are represented in Fig. 9 and Table 2. Fig. 9 displays the overall result of operating the cooling system with solar energy.

Following sunrise at 05:10, the outlet collector water temperature began to rise rapidly, energizing the system. The tank valves were opened at 08:30 (478 W m^{-2}) and at 08:50 (543 W m^{-2}) the collector outlet temperature was 2 °C higher than the average tank temperature. The generator pump was switched on immediately afterwards to allow the transfer of stored heat in the tank from the previous day's operation to raise the temperature of the LiBr solution to it's boiling point at about 59 °C inside the generator. This occurred when the hot water temperature entering the generator was 65 °C. Cooling was realized at 09:40 solar time, when the chilled water temperature leaving the evaporator began to drop rapidly and was supplied to the FCUs until 18:20. Therefore, 4.5 h of solar insolation falling on the collectors could not be utilized to produce cooling. The grey area under the curve of the heat input to the evaporator on Fig. 9 shows the actual cooling produced. At 08:30, heat was supplied to the storage tank. From then on, no cooling was produced for 1 h and 10 min. The insolation from sunrise to 08:30 is necessary to overcome thermal inertia in the system. In this period, the collector outlet temperature increased up to top of the tank temperature. From then until 16:30, the flat-plate collectors supplied heat to the storage tank, which in turn supplied heat to the generator. From 16:40 to sunset, the insolation was not useful for the process, since it was insufficient to add heat to the tank. The white area under the curve of the storage tank represents the total heat lost from the system from 05:10 to 08:30; from 08:30 to 16:40 and from 16:40 to 19:12, 5.5 kW h m^{-2} day^{-1}. From 08:30 to 18:20, the hatched area above the generator curve represents the heat input to generator. From 08:30 to 16:30, the cross-hatched area represents the simultaneous process of heat delivered to the generator and supplemented from the collector array. From 16:30 to 18:20, the generator was supplied with heat stored in the tank and no heat was supplemented to the tank from the collector array. At 14:30, the heat input to the tank became approximately equal to the heat output of it. From 17:40 to 18:20, the absorption machine operated in transient regime. The transient regime was reached when the hot water temperature difference reduced to less than 1 °C. The absorption chiller was operated from 09:40 to 18:20, a total 8 h and 40 min (approximately two third the sunshine time). This describes a typical day of solar cooling in Madrid.

The absorption cooling process was analysed in detail by representing the heat inputs and outputs to the machine on a diagram to establish a heat balance as shown in Fig. 10. Eqs. (9)–(11) were used to calculate the generator, evaporator and condenser plus absorber heat loads. The heat input to the chiller at the generator and evaporator was found to be

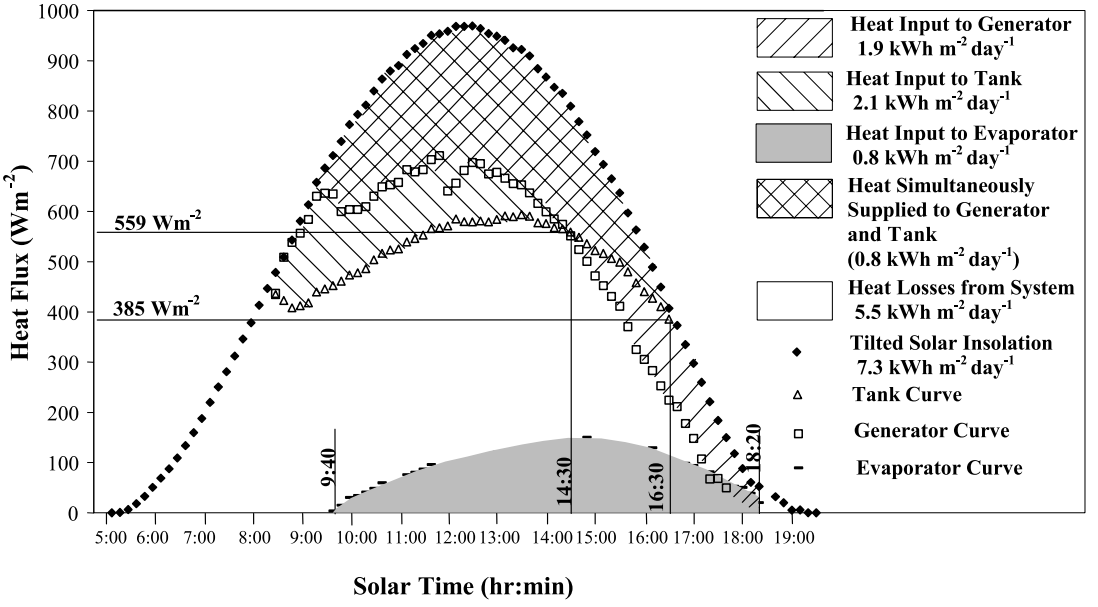

Fig. 9. Heat flows encountered during the conversion of solar insolation into cold (08/08/2003).

Table 2
Daily and period energy balance for the solar cooling system (25/07/03–19/08/03)

July–August 2003	Daily G_T (kW h day^{-1})	Daily $\dot{Q}_e$ (kW h day^{-1})	Daily $\dot{Q}_g$ (kW h day^{-1})	Daily $\dot{Q}_c + \dot{Q}_a$ (kW h day^{-1})	Daily $\dot{Q}_{fpc}$ (kW h day^{-1})	Daily $\dot{Q}_{t,input}$ (kW h day^{-1})	Daily $\dot{Q}_{t,stored}$ (kW h day^{-1})	Daily ave. η_{fpc} (–)	Daily ave. COP (–)	Daily ave. $Q_{t,input}/G_T$ (–)	Daily ave. Q_g/G_T (–)	Daily ave. SCR (–)
25	366.7	35.0	99.5	126.5	194.0	111.3	124.6	0.53	0.35	0.30	0.27	0.10
26	355.3	26.9	92.2	113.6	194.6	106.6	116.4	0.55	0.29	0.30	0.26	0.08
27	357.3	23.0	95.0	107.0	175.3	106.6	125.2	0.49	0.24	0.30	0.27	0.06
29	353.2	26.9	94.5	110.8	178.4	108.5	122.3	0.51	0.28	0.31	0.27	0.08
30	328.5	30.6	84.1	108.2	175.3	93.0	107.1	0.53	0.36	0.28	0.26	0.09
31	358.0	32.6	87.3	115.5	183.7	104.9	105.1	0.51	0.37	0.29	0.24	0.09
2	321.3	31.9	86.9	112.5	170.1	98.1	119.5	0.53	0.37	0.31	0.27	0.10
5	342.9	34.8	90.5	119.2	180.1	103.1	125.6	0.53	0.38	0.30	0.26	0.10
6	354.7	33.6	84.1	112.3	179.4	97.7	117.4	0.51	0.40	0.28	0.24	0.09
8	364.1	40.0	95.9	129.4	183.4	106.7	132.1	0.50	0.42	0.29	0.26	0.11
10	326.0	25.4	73.3	91.1	168.6	92.2	100.5	0.52	0.35	0.28	0.22	0.08
11	344.3	35.3	87.1	117.6	178.0	102.7	119.8	0.52	0.41	0.30	0.25	0.10
12	348.7	24.4	83.2	98.0	180.8	100.4	114.7	0.52	0.29	0.29	0.24	0.07
13	349.3	21.2	92.1	105.0	179.2	102.1	123.8	0.51	0.23	0.29	0.26	0.06
14	328.0	18.2	69.8	82.6	174.7	86.3	94.3	0.53	0.26	0.26	0.21	0.06
15	329.2	19.3	79.5	91.8	172.6	90.0	109.2	0.52	0.24	0.27	0.24	0.06
16	336.1	35.2	85.6	111.2	170.2	99.0	116.4	0.51	0.41	0.29	0.25	0.10
17	346.5	26.6	83.7	101.2	178.6	97.1	115.4	0.52	0.32	0.28	0.24	0.08
18	376.3	38.9	94.6	122.6	198.2	113.6	127.3	0.53	0.41	0.30	0.25	0.10
19	354.9	37.6	91.3	117.4	187.8	110.1	125.1	0.53	0.41	0.31	0.26	0.11
Period ave.	347.1	29.9	87.5	109.7	180.1	101.5	117.1	0.52	0.34	0.29	0.25	0.09

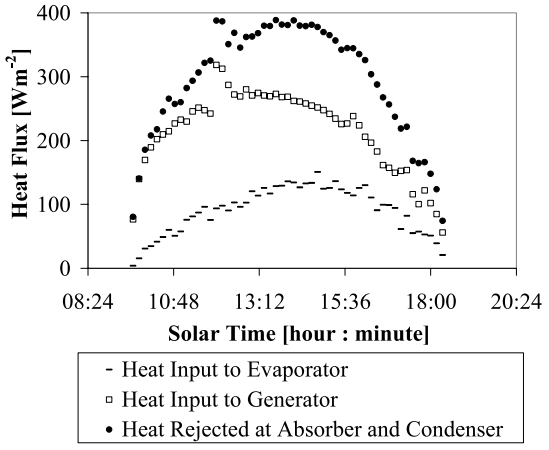

Fig. 10. Heat flows in the absorption cooling process against solar time (08/08/2003).

approximately equal to the sum of the heat rejected at the condenser and absorber. The heat flows were not exactly balanced due to the heat loss from the absorption machine, since the refrigeration process was non-adiabatic. The daily heat lost from the absorption machine heat exchangers was found to be 6.5 kW h day^{-1} or 0.13 kW h m^{-2} day^{-1}. This amounts to 6.8% of heat input to generator. In contrast, the bulk of the heat lost from the whole system was found to be associated with the difference between the incident solar energy from sunrise to sunset of 364.1 kW h day^{-1} or 7.3 kW h m^{-2} day^{-1} and the heat input to generator of 95.9 kW h day^{-1} or 1.92 kW h m^{-2} day^{-1}. Thus the total heat lost from the system was found to be 274.7 kW h day^{-1} or 5.5 kW h m^{-2} day^{-1} as shown in Fig. 9. The heat losses can be evaluated from Table 2.

Fig. 11 displays the refrigeration coefficient of performance obtained by applying Eq. (13), which varied from as low as 0.05 at the start of the cooling period to 0.63 at 17:00 on 08/08/03. The average COP for the day was 0.42. The low COP at the beginning and end of the day can be explained from the fact that the cooling capacity at these

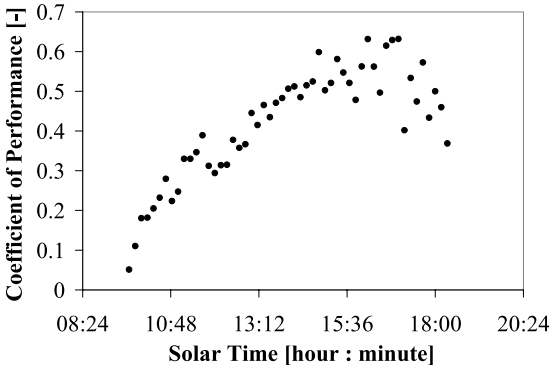

Fig. 11. Coefficient of performance of the absorption cooling process against solar time (08/08/2003).

times was extremely low compared with the generator heat load due to the transient behavior exhibited by the chiller and its heat losses.

The instantaneous solar cooling ratio (SCR) is a system efficiency parameter and was evaluated from the ratio of cooling produced and the solar radiation incident on the tilted plane of the collectors given by the following relation:

$$\mathrm{SCR} = \frac{q_e}{G_T} \tag{15}$$

Fig. 12 represents the instantaneous SCR data plotted from 09:40 to 18:20. Daily cooling output and daily insolation were also evaluated in kW h day^{-1} for the collector area of 49.9 m^2 and the ratio of the two provided the daily average SCR given in Table 2. A daily average SCR of 11% was determined for the duration of cooling produced from the total sunshine hours on the day in question. SCR was found to increase strongly under two environmental conditions: high dry bulb temperature and low relative humidity. At a high ambient dry bulb temperature, lower collector heat loss was realised, resulting in higher collector efficiency. At a low relative humidity (low wet bulb temperature), higher cooling tower performance was realised, due to which lower absorption and condensation temperatures were obtained, which enhanced the COP of the chiller. This proves that the overall performance of the technology is highly dependent on environmental parameters and it works best in dry and hot summers such as that of Madrid.

7. Energy balance for the installation

Table 2 shows the daily energy balance for the installation during the entire monitoring period. The data consists essentially of 12 parameters relating to energy flows for the 49.9 m^2 of collector (absorber) area in addition to efficiency measures. The minimum to maximum daily values of these parameters are as follows:

– Tilted solar insolation: 321.3–376.3 kW h day^{-1}.

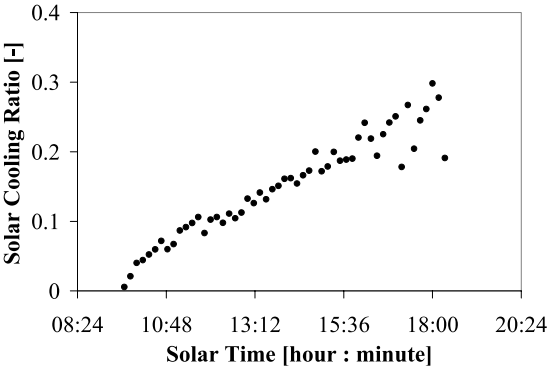

Fig. 12. Solar cooling ratio against solar time (08/08/2003).

- Heat input to evaporator: 18.2–40.0 kW h day^{-1}.
- Heat input to generator: 69.8–99.5 kW h day^{-1}.
- Heat rejected at condenser and absorber: 82.6–129.4 kW h day^{-1}.
- Heat output of flat-plate collectors: 168.6–198.2 kW h day^{-1}.
- Heat input to tank: 86.3–113.6 kW h day^{-1}.
- Heat stored in tank: 94.3–132.1 kW h day^{-1}.
- Efficiency of flat-plate collectors (without considering losses in pipes and plate heat exchanger): 0.49–0.55.
- Coefficient of performance of absorption chiller: 0.23–0.42.
- Ratio of heat input to tank and tilted solar insolation: 0.26–0.31.
- Ratio of heat input to generator and tilted solar insolation: 0.21–0.27.
- Solar cooling ratio: 0.06–0.11.

Over the period of 20 days of monitoring (25/07 to 19/08), the following results were achieved:

- Total solar energy intercepted was 139 kW h m^{-2}.
  Total solar energy supplied to the generator was 35.1 kW h m^{-2}.
- Total cold produced was 12 kW h m^{-2}.
- Period average refrigeration COP was 0.34.
- Period average solar cooling ratio was 0.09.

8. Conclusions

A solar cooling system consisting of a flat-plate collector array, absorption machine, cooling tower and hot water storage tank was demonstrated under real time conditions in Leganés 20 km Southwest of Madrid. The system worked entirely with solar energy and produced chilled water for 7.33 h (under permanent regime) on a hot day of 8th August 2003. The highest cooling energy was delivered on this day. The chiller operated in transient regime for 1.34 h (1.17 h for start-up and 0.17 h for shut-down). Data for this day has been plotted on a novel diagram showing energy flows in the solar cooling system. This diagram provides a clear indication of the total heat losses in the solar cooling process.

Table 1 summarises the results for the monitored day of 8th August 2003. It gives the solar times, system temperatures and solar insolation at which the main processes occurred: start and end of cold production, start and end of heat input to storage tank, equal tank heat input and output, maximum cooling capacity and COP.

For the monitored day, the following efficiencies were obtained:

- Daily average collector efficiency (without considering pipe and plate heat exchanger losses) was 0.50.
- Daily average ratio of heat input to tank and solar insolation was 0.29.
- Daily average ratio of heat input to generator and solar insolation was 0.26.
- Daily average COP was 0.42.
- Daily average solar cooling ratio was 0.11.

To improve the solar cooling ratio, it is recommended that thicker tank insulating material be used such that an overall heat loss coefficient of about 0.8 W m^{-2} K^{-1} can be achieved. Also, the steel pipes should be replaced with UPVC (plastic) pipes in the primary and tertiary circuits.

A primary circuit bypass should be provided to allow the collector water to mix with the storage tank water when the system does not contain antifreeze additive, to avoid the high heat losses at the plate heat exchanger.

The main lessons learned were:

- High thermal lag.
- High heat losses at storage tank, pipes and plate heat exchanger.
- Large penalty in cooling capacity.
- Moderate refrigeration COP.

COP could be improved by considering a customized low heat medium temperature driven commercially available single-effect ($LiBr/H_2O$) absorption chiller design of smaller nominal capacity [7].

The data presented in the paper can be used as benchmark figures for comparative purposes. For instance, mathematical models can be validated. Also, the performance of other similar installations operating in similar climatic conditions can be predicted.

Acknowledgements

The authors are grateful to Prof T.G. Karayiannis of London South Bank University for supporting this research collaboration between five participating organizations. Our thanks are also extended to C. Marugan and the academic and technical staff at UC3M particularly Dr M. Venegas, Dr M. Vega, M. Sardina and S. López. The valuable contribution of working knowledge of the installation by E. Martin of IETcc is gratefully acknowledged. Acknowledgements are also to ATYCA Program of the Ministerio de Industria of Spain, the Consejería de Medioambiente de la Comunidad de Madrid and London South Bank University for the financial support.

References

[1] R. Chung, J.A. Duffie, G.O.G. Löf, A study of a solar air-conditioner, Mech Eng 85 (31) (1963).
[2] N.R. Sheridan, Performance of the Brisbane solar house, Proceedings of the ISES conference, International Solar Energy Society, Melbourne, Australia, 1970.

[3] M. Izquierdo, D. Tinaut, Instalación de refrigeración con colector plano de energía solar (in Spanish). El Instalador; 1984, Monografía No 17:121–6, España.
[4] M. Izquierdo, D. Tinaut, Solar-heated absorption system: experimental results for summer period 1984. In: Ponencian, Poster and Proceedings of the XXIII Renc Int COMPLES: la Energía Solar en la Cooperación Norte-Sur; 1985, Sevilla, España: 427–32.
[5] Z.F. Li, K. Sumathy, Experimental studies on a solar powered air-conditioning system with partitioned hot water storage tank, Sol Energy 71 (5) (2001) 285–297.
[6] N.K. Vegen, S. Furbo, L.J. Shah, Development of a 12.5 m^2 solar collector panel for solar heating plants, Sol Energy Mater Sol Cells 84 (2004) 205–223.
[7] J. Scharfe, New generation absorption chillers. ABO Newsletter No. 5: international energy agency heat pump programme—annex 24: absorption machines for heating and cooling in future energy systems, UK; 1999.
[8] A. Syed, G.G. Maidment, R.M. Tozer, J.F. Missenden, A study of the economic perspectives of solar cooling schemes, Proceedings of the CIBSE national technical conference, Chartered Institution of Building Services Engineers, London, 2002. www.cibse.org.
[9] ASHRAE Equipment Handbook, American society of heating, refrigerating and air-conditioning engineers, Atlanta, GA, USA 1988.
[10] W.S. Duff, R. Winston, J.J. O'Gallagher, T. Henkel, J. Muschaweck, R. Christiansen, J. Bergquam, Demonstration of a new type of ICPC design with a double-effect absorption chiller in an office building in Sacramento, California, Proceedings of the ASES Solar 99 conference, American Section of the International Solar Energy Society, Portland, Maine, 1999. p. 175–179.
[11] A. Syed, G.G. Maidment, R.M. Tozer, J.F. Missenden, An economic investigation of solar energy applied to water cooled liquid chillers, Proceedings of SET 02, Sustainable Energy Technologies, Porto, 2002. RHP 40/70-44-70.
[12] International energy agency task 25: solar assisted air-conditioning of buildings. Web resource: http://www.iea-shc.org/task25/.
[13] P. Lamp, F. Ziegler, European research on solar-assisted air-conditioning, Int J Refrigeration 21 (2) (1998) 89–99.
[14] Solartechnik Prüfung Forschung (SPF) Info-CD 2002. Viessmann Vitosol 100 (2.5 m^2) Collector Test Report, Institut für Solartechnik, Hochschule, Rapperswil HSR, Oberseestrasse 10, CH-8640, Rapperswil, Switzerland.
[15] H.W. Coleman, Steele Jr, Experimental uncertainty analysis for engineers, Wiley, New York, 1999. ISBN: 0471121460.
[16] E. Mathioulakis, K. Voropoulos, V. Belessiotis, Assessment of uncertainty in solar collector modeling and testing, Sol Energy 66 (5) (1999) 337–347.
[17] Kipp, Zonen. Instruction manual: pyranometer CM 6B/7B. Delft, The Netherlands; 2001.
[18] V. Sabatelli, D. Marano, G. Braccio, V.K. Sharma, Efficiency test of solar collectors: uncertainty in the estimation of regression parameters and sensitivity analysis, Energy Convers Manage 43 (2002) 2287–2295.
[19] Yazaki Energy Systems, Catalogue data on absorption chiller model (WFC-10) 1997.
[20] R.M. Tozer, M.A. Lozano, Thermo-economic optimisation of a single-effect absorption chiller and cooling tower, Proceedings of the ISHPC 99 conference, International Sorption Heat Pump Conference, Munich, 1999. p. 1–7.
[21] IEA Heat Pump Programme (Annex 24), Absorption machines for heating and cooling in future energy systems, HPP-AN24-4 (final report); 2000, p. 30–1.
[22] J.A. Duffie, W.A. Beckman, Solar engineering of thermal processes, Wiley, New York, 1991. ISBN: 0471510564.